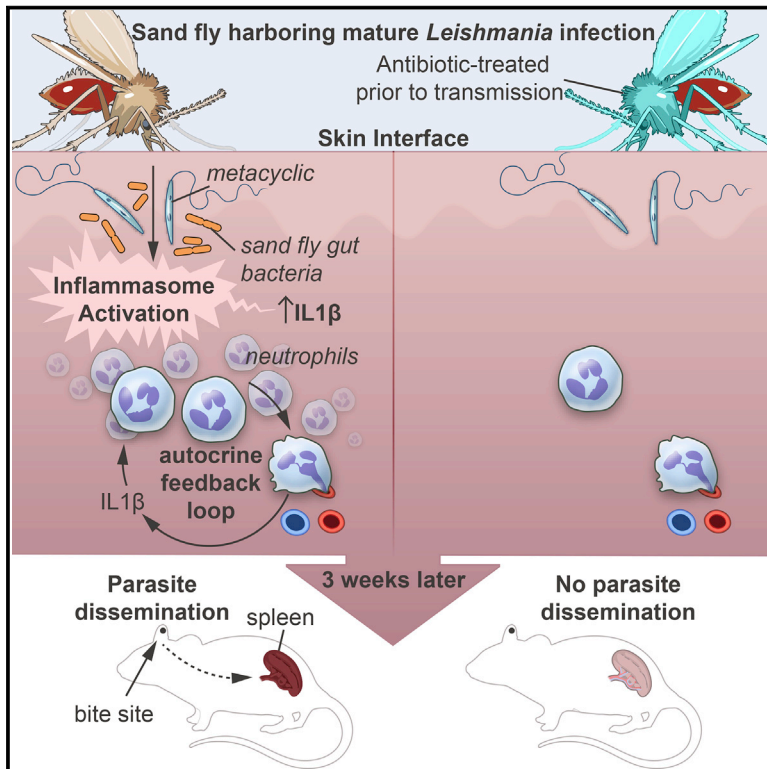# Cell Host & Microbe

Gut Microbes Egested during Bites of Infected Sand Flies Augment Severity of Leishmaniasis via Inflammasome-Derived IL-1β

Graphical Abstract

Authors

Ranadhir Dey, Amritanshu B. Joshi, Fabiano Oliveira, ..., Hira L. Nakhasi, Jesus G. Valenzuela, Shaden Kamhawi

Correspondence

jvalenzuela@niaid.nih.gov (J.G.V.),
skamhawi@niaid.nih.gov (S.K.)

In Brief

<para>Neutrophils recruited to sand fly bite sites shelter *Leishmania*, augmenting disease. Dey et al. demonstrate that egestion of sand fly gut microbes into host skin primes the inflammasome to produce IL-1β, which sustains neutrophil recruitment. Removing gut microbiota or blocking IL-1β before transmission abolishes neutrophil recruitment and impairs *Leishmania* dissemination.</para>

Highlights

- Gut microbes egested by *Leishmania*-infected sand flies prime the host inflammasome

- Inflammasome-derived IL-1β sustains recruitment of neutrophils to bite sites

- Giving antibiotics to sand flies before transmission abolishes neutrophil infiltration

- Abolishing neutrophil infiltration at bite sites impairs *Leishmania* dissemination

CellPress

Gut Microbes Egested during Bites of Infected Sand Flies Augment Severity of Leishmaniasis via Inflammasome-Derived IL-1β

Ranadhir Dey,[1] Amritanshu B. Joshi,[1] Fabiano Oliveira,[2] Lais Pereira,[2,3] Anderson B. Guimarães-Costa,[2] Tiago D. Serafim,[2] Waldionê de Castro,[2] Iliano V. Coutinho-Abreu,[2] Parna Bhattacharya,[1] Shannon Townsend,[2] Hamide Aslan,[2] Alec Perkins,[2] Subir Karmakar,[1] Nevien Ismail,[1] Morgan Karetnick,[2] Claudio Meneses,[2] Robert Duncan,[1] Hira L. Nakhasi,[1] Jesus G. Valenzuela,[2,*] and Shaden Kamhawi[2,4,*]

[1]Laboratory of Emerging Pathogens, Division of Emerging and Transfusion Transmitted Diseases, Center for Biologics Evaluation and Research, Food and Drug Administration, Silver Spring, MD 20993, USA
[2]Vector Molecular Biology Section, Laboratory of Malaria and Vector Research, National Institute of Allergy and Infectious Diseases, National Institutes of Health, Rockville, MD 20852, USA
[3]Department of Molecular Microbiology and Immunology, Johns Hopkins Bloomberg School of Public Health, Baltimore, MD 21205, USA
[4]Lead Contact
*Correspondence: jvalenzuela@niaid.nih.gov (J.G.V.), skamhawi@niaid.nih.gov (S.K.)
https://doi.org/10.1016/j.chom.2017.12.002

SUMMARY

Leishmania donovani parasites are the cause of visceral leishmaniasis and are transmitted by bites from phlebotomine sand flies. A prominent feature of vector-transmitted *Leishmania* is the persistence of neutrophils at bite sites, where they protect captured parasites, leading to enhanced disease. Here, we demonstrate that gut microbes from the sand fly are egested into host skin alongside *Leishmania* parasites. The egested microbes trigger the inflammasome, leading to a rapid production of interleukin-1β (IL-1β), which sustains neutrophil infiltration. Reducing midgut microbiota by pretreatment of *Leishmania*-infected sand flies with antibiotics or neutralizing the effect of IL-1β in bitten mice abrogates neutrophil recruitment. These early events are associated with impairment of parasite visceralization, indicating that both gut microbiota and IL-1β are important for the establishment of *Leishmania* infections. Considering that arthropods harbor a rich microbiota, its potential egestion after bites may be a shared mechanism that contributes to severity of vector-borne disease.

INTRODUCTION

Vector-borne diseases account for more than a billion new infections and more than a million deaths each year (WHO, 2014). Transmission of a variety of pathogens by bites of their arthropod vectors enhances pathogen establishment and disease severity (Cox et al., 2012; Liu and Bonnet, 2014; Peters et al., 2008; Pingen et al., 2016). Enhancement of disease following transmission of viruses by mosquitoes (Pingen et al., 2016) or *Leishmania* parasites by sand flies (Peters et al., 2008) has been associated to neutrophil-driven inflammation. Neutrophils are first responders

to sites of skin injury and are a vital part of wound healing (de Oliveira et al., 2016). Therefore, their arrival at the bite site is partly driven by tissue damage caused by insect probing and biting. Yet mosquito or sand fly bites augment the response of neutrophils with consequences for pathogen establishment (Peters et al., 2008; Pingen et al., 2016). However, the mechanism driving sustained recruitment of neutrophils after vector bites has not been fully elucidated.

Leishmaniasis, a vector-borne disease transmitted by bites of phlebotomine sand flies, encompasses a spectrum of diseases that range from self-healing cutaneous leishmaniasis to disseminating visceral leishmaniasis (VL). VL caused by *Leishmania donovani* in the Indian subcontinent and East Africa has a high fatality rate in untreated patients with patent infections. Following natural transmission by sand fly bites, *L. donovani* parasites migrate from the skin to the liver and spleen, damaging organs, yet mediators of parasite dissemination from the bite site remain unknown.

Several vector-derived components of insect and parasite origin including saliva, proteophosphoglycans, and exosomes, are regurgitated into the bite site and modulate the host immune response in favor of parasite survival (Atayde et al., 2015; Gomes and Oliveira, 2012; Rogers, 2012). Using a VL mouse model of vector-transmitted *L. donovani*, our data indicate that sand fly gut microbes are egested into host skin where it triggers the inflammasome and amplifies interleukin-1β (IL-1β) production by neutrophils. IL-1β then acts as an early autocrine signal to sustain an intense recruitment of neutrophils to bite sites. Furthermore, we show that the microbe-initiated immune response sanctions downstream events that govern dissemination of *L. donovani*.

RESULTS

Vector-Transmitted *L. donovani* Disseminates from the Skin to the Spleen

Twenty *L. donovani*-infected sand flies harboring transmissible infections (Figure S1A) reproducibly transmit about 10^3–10^4
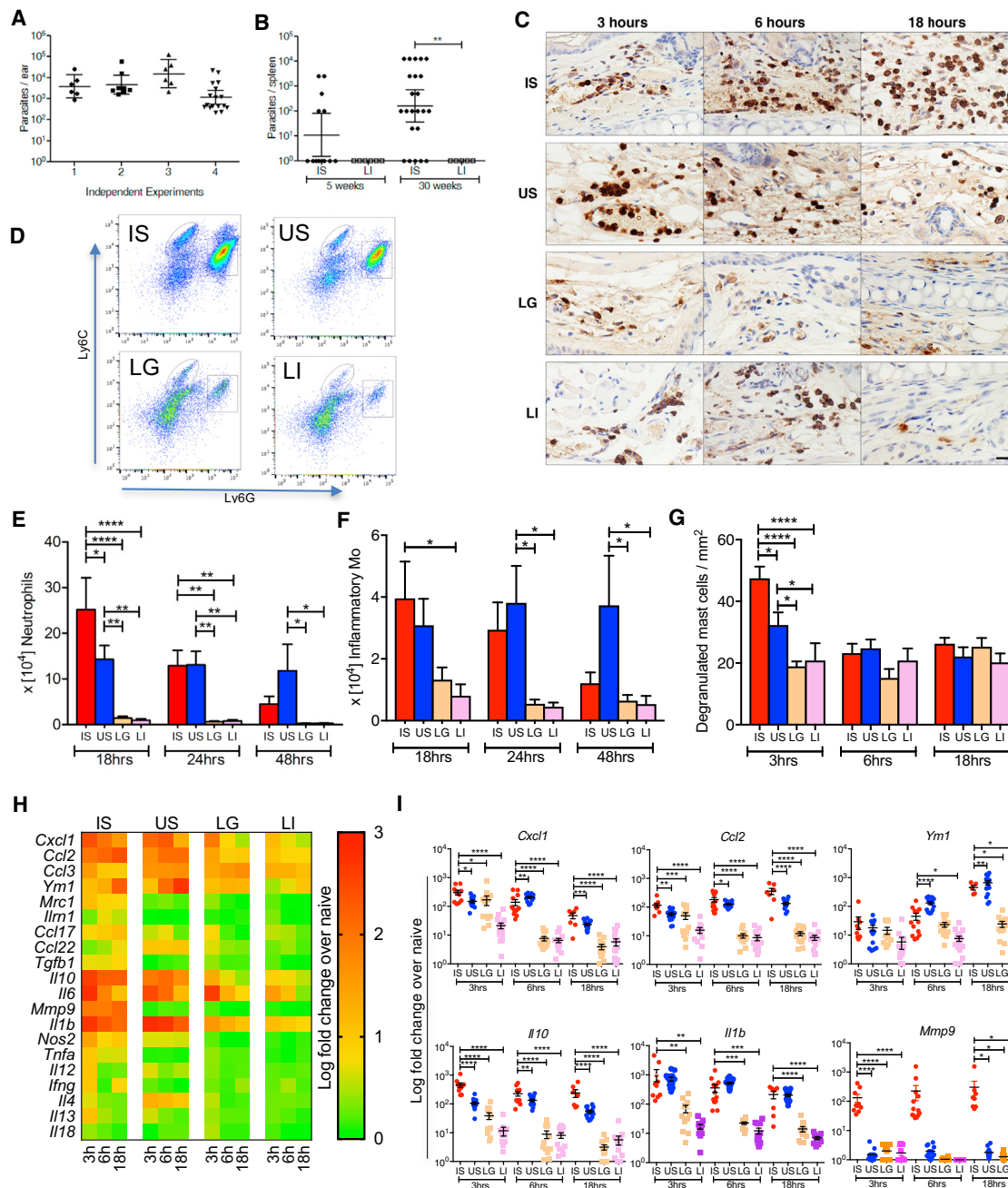
Figure 1. The Inflammatory Response at the Bite Site of Vector-Transmitted *L. donovani* Parasites

(A) Parasite burden determined by qPCR in individual mouse ears immediately after exposure to 20 infected sand flies (n ≥ 6 mouse ears per experiment).

(B) Parasite burden in individual mouse spleens was determined by serial dilution at 5 and 30 weeks after exposure to 20 infected sand flies (IS) belonging to the same group or to an intradermal injection of 10^5 metacyclic parasites (LI). Data are pooled from two independent experiments (n ≥ 13 for IS, n ≥ 5 mice for LI).

(C–I) Mouse ears 3–48 hr after exposure to 20 IS, 20 uninfected sand flies (US), intradermal co-inoculation with LI plus extract of one salivary gland (LG), and LI. (C) Mouse ear sections stained with anti-Gr1 antibody. Pictures are representative of four independent experiments (n ≥ 4 mouse ears per condition per time point). Scale bar, 20 μm. (D–F) Cells recovered from individual mouse ears were stained for flow cytometry. Data are representative of two independent experiments (n = 6 mouse ears per condition per time point). (D) Representative plots of Ly6G and Ly6C expression distinguish neutrophils (square gate) and inflammatory monocytes (oval gate) graphed in (E) and (F), respectively. (G) Degranulated mast cells in at least six fields counted from ear sections stained with toluidine blue. Data are representative of four independent experiments (n ≥ 5 mouse ears per condition per time point). (H and I) mRNA expression of inflammatory mediators produced in mouse ears determined by qPCR. Data are pooled from more than three independent experiments (n ≥ 7 mouse ears per condition per time point). (H) Heatmap of the global inflammatory skin response. (I) Expression profile of distinct genes relevant to the inflammatory response after IS.

parasites to mouse ears (Figures 1A and S1B). A mean ± SD of 7.14 ± 4.47 *L. donovani* fed flies per ear (Figure S1C) result in parasite dissemination from the skin to the spleen by 5 weeks after vector transmission (Figure 1B). After 30 weeks, 18 of 23 mice had splenic parasites, with a geometric mean ± SD of $3.98 \times 10^3 \pm 5,506$ parasites per spleen in positive mice. In contrast, 10^5 culture-derived metacyclics injected intradermally fail to visceralize (Figure 1B), affirming the heightened severity of vector-transmitted leishmaniasis.

Next, we explored the early innate immune response after an *L. donovani*-infected sand fly bite (IS), an uninfected sand fly bite (US), intradermal co-inoculation of *L. donovani* parasites and salivary gland sonicate (LG), or intradermal *L. donovani* injection (LI) from 3 hr up to 48 hr. Immunohistochemical (IHC) analysis of ear sections and flow cytometry gated on neutrophils and inflammatory monocytes (Figure S2A) recovered from ear cells established the intense and persistent nature of neutrophil recruitment to bite sites up to 48 hr following IS or US, compared with a weak and transient infiltration after LG or LI (Figures 1C–1E), reproducing findings following vector transmission of *Leishmania major* (Peters et al., 2008). Although neutrophil recruitment was generally similar after IS and US, it was significantly higher at 18 hr after IS (Figures 1C and 1E), potentially due to parasites or to the promastigote secretory gel and exosomes, both reported to attract neutrophils (Rogers, 2012; Silverman and Reiner, 2011). Monocyte recruitment was not observed up to 6 hr (data not shown), but was significantly higher at 18 hr after IS compared with LG and LI (Figure 1F). Interestingly, the number of recruited neutrophils and inflammatory monocytes per ear after IS compared with US was augmented by correcting for fed flies, becoming significant for monocytes at 18 hr (Figure S2B). Generally, US are unhampered by infection with *Leishmania* and tend to feed more easily.

Another striking difference among the groups was a significant increase in the number of degranulated mast cells 3 hr after IS compared with US, LG, and LI, with US inducing an intermediate response (Figures 1G, S2C, and S2D). Mast cells release mediators that promote and qualify the innate immune response, and have been implicated in production of CXCL1 and matrix metalloprotease 9 (MMP9) and the early recruitment of neutrophils (Chiba et al., 2015; De Filippo et al., 2013).

At the transcriptional level, *Cxcl1* and *Ccl2* chemokines, critical for recruitment of neutrophils and monocytes, respectively (De Filippo et al., 2013; Shi and Pamer, 2011), several markers of alternatively activated M2 monocytes/macrophages (Mo/MΦ) (Murray and Wynn, 2011; Porta et al., 2009; Sica et al., 2014) associated with wound healing and the inability to kill *Leishmania* parasite (Murray and Wynn, 2011; Rogers, 2012), and the cytokines *Il10* and *Il1b* were expressed at significantly higher levels after IS compared with LG and LI (Figures 1H and 1I). Interestingly, *Mmp9* was induced at significantly higher levels after IS compared with all other groups (Figures 1H and 1I). Apart from digestion of the extracellular matrix, *Mmp9* has been associated with intense recruitment of neutrophils (Bradley et al., 2012) and

orchestrating a positive feedback loop for neutrophil recruitment to sites of inflammation (Opdenakker et al., 2001).

Infected Sand Fly Bites Activate the NLRP3 Inflammasome

Of pivotal significance, the sustained high induction of *Il1b* at 3–18 hr after IS and US compared with LI (Figures 1H and 1I) suggested that infected and uninfected sand fly bites may activate the inflammasome (Guo et al., 2015). A parallel induction of higher levels of *Tnfa*, *Nos2*, and *Ifng* after IS compared with LG and LI (Figure 1H) further supported our hypothesis (Guo et al., 2015; Lima-Junior et al., 2013).

IL-1β is tightly regulated at the transcriptional and translational levels, and by proteolytic processing (Guo et al., 2015; Radwan et al., 2010). To understand the biological relevance of *Il1b* induction after sand fly bites, we assessed its protein levels in ear tissue lysates at 6 hr after IS and US. Unexpectedly, the IL-1β protein level was significantly higher after IS compared with US (Figure 2A). This was supported by IHC staining directed against mature soluble IL-1β (Figure 2B). Notably, neutrophils were the main source of IL-1β in mouse ears at 6 hr after IS and showed a 37-fold increase in their number compared with resting skin (Figures 2C–2E). Six hours after bites, the protein levels of NLRP3, pro-caspase-1, and cleaved caspase-1 were also reduced after US compared with IS (Figure 2F and Table S1). Importantly, after immunoprecipitation using apoptosis-associated speck-like protein containing a CARD domain (ASC), NLRP3 detection was considerably stronger after IS compared with US (Figure 2G and Table S1) signifying a more efficient assembly of the inflammasome after IS. Consistent with these conclusions, *Nlrp3* expression was significantly higher while expression of *Ifnb*, an inhibitor of the NLRP3 inflammasome (Guarda et al., 2011; Guo et al., 2015), was reduced after IS compared with US over the timeline of the study (Figure 2H). Apoptotic cells that contribute to inflammasome activation (Shimada et al., 2012) and promote an anti-inflammatory environment (Ribeiro-Gomes and Sacks, 2012) were also more prevalent in ear sections after IS compared with US (Figure 2I).

Since *Leishmania* species have been reported to activate the NLRP3 inflammasome (Charmoy et al., 2016; Gurung et al., 2015; Lima-Junior et al., 2013), we incubated lipopolysaccharide (LPS)-primed bone marrow-derived macrophages (BMDM) with stationary-phase *L. donovani* parasites. High levels of mature IL-1β were only produced in the presence of LPS, while parasites alone induced IL-10 production (Figure 2J). Nevertheless, increasing the number of parasites incubated with presence of LPS-primed cells significantly elevated IL-1β secretion (Figure 2J) indicating that *Leishmania* contributes to activation of the inflammasome.

Gut-Residing Microbes Are Co-egested alongside *Leishmania* Parasites during Infected Sand Fly Bites

Induction of high levels of IL-1β after IS and US led us to hypothesize that midgut microbes, reported from wild-caught and

---

Statistical significance (*p < 0.05, **p < 0.01, ***p < 0.001, ****p < 0.0001) was calculated using the Wilcoxon ranked sum test (A and B) and one-way ANOVA followed by a Holm-Sidak multiple comparisons test (E–G and I). Error bars in (A) and (B) indicate the geometric mean with 95% confidence interval. Error bars in (E) to (G) and (I) indicate the mean ± SEM.
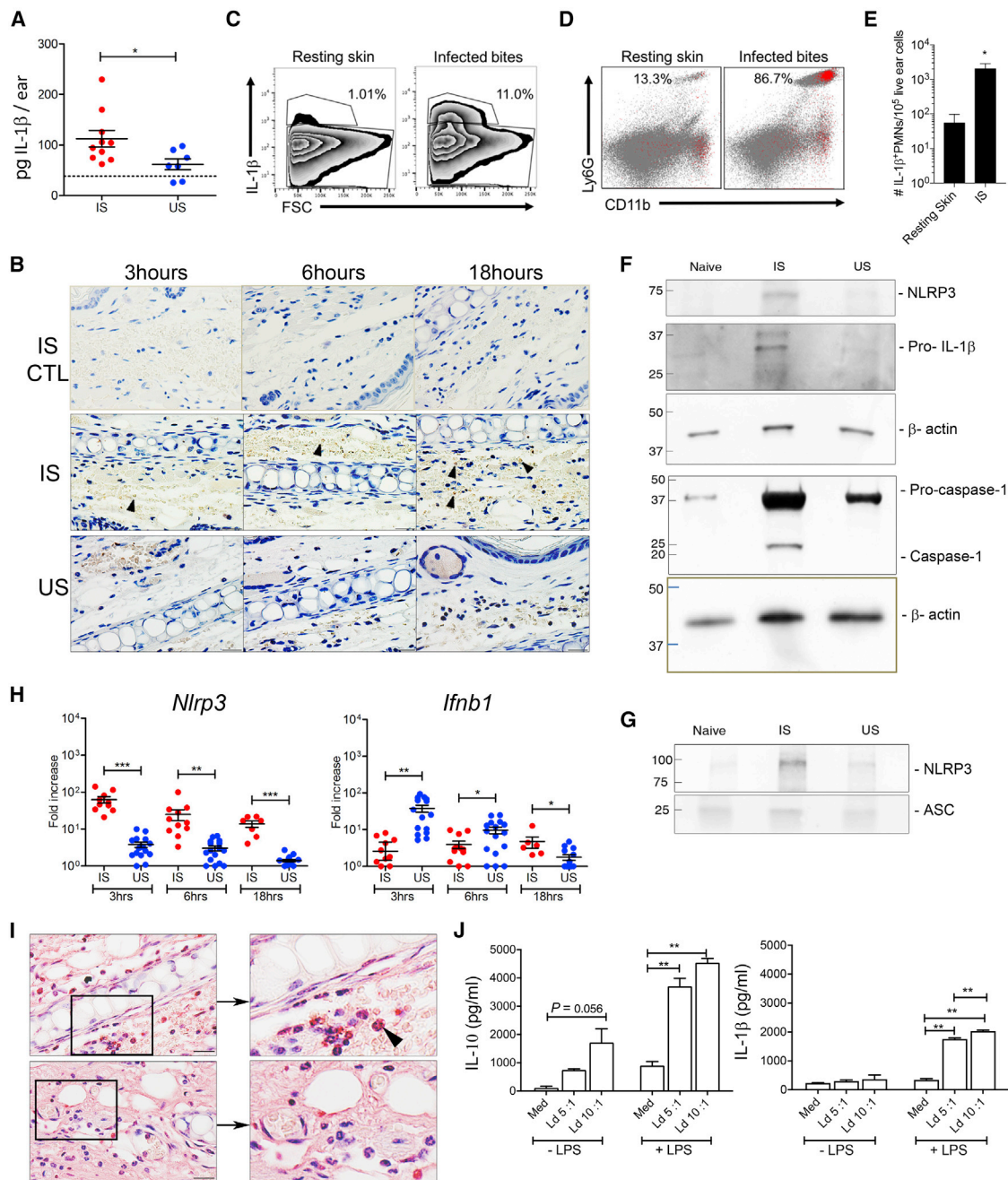See also Figures S1–S3.

Figure 2. *L. donovani*-Infected Sand Fly Bites Activate the NLRP3 Inflammasome in Neutrophils

In (A), (C) to (G), and (I), mouse ears were processed 6 hr after exposure to 20 infected (IS) or uninfected (US) sand flies.

(A) *Ex vivo* IL-1β protein levels from ear lysates measured by ELISA. Data are representative of two independent experiments (n ≥ 7 mouse ears per condition). Dotted line represents the mean ± SEM of endogenous IL-1β levels in naive samples.

(B) Mouse ear sections stained with either anti-IL-1β antibody targeting the mature protein or its isotype control (CTL) at 3–18 hr after IS or US. Pictures are representative of two independent experiments (n = 2 mouse ears per condition per time point). Arrowheads indicate IL-1β-secreting cells. Scale bars, 20 μm.

(C–E) Cells recovered from mouse ears after IS were stained for flow cytometry. Representative plots of IL-1β+ cells (C) back-gated (red) onto LY6G+/CD11b+ neutrophils (D). (E) The number of IL-1β+ neutrophils per 10^5 ear cells from two independent experiments (n = 6 mouse ears per condition).

(F) Representative western blot of NLRP3, caspase-1, and pro-IL-1β protein levels after IS and US (n = 4 mouse ears per condition).

(G) Representative western blot of NLRP3 protein levels after immunoprecipitation using anti-ASC antibody (n = 2 mouse ears per condition).

(H) *Nlrp3* and *Ifnb* mRNA expression determined by qPCR at 3–18 hr after IS or US. Data are pooled from three independent experiments (n ≥ 7 mouse ears per condition per time point).

(I) Mouse ear sections stained with TUNEL. Pictures are representative of two independent experiments (n = 3 mouse ears per condition). Boxed area is magnified to highlight apoptotic cells (arrowhead). Scale bars, 20 μm.
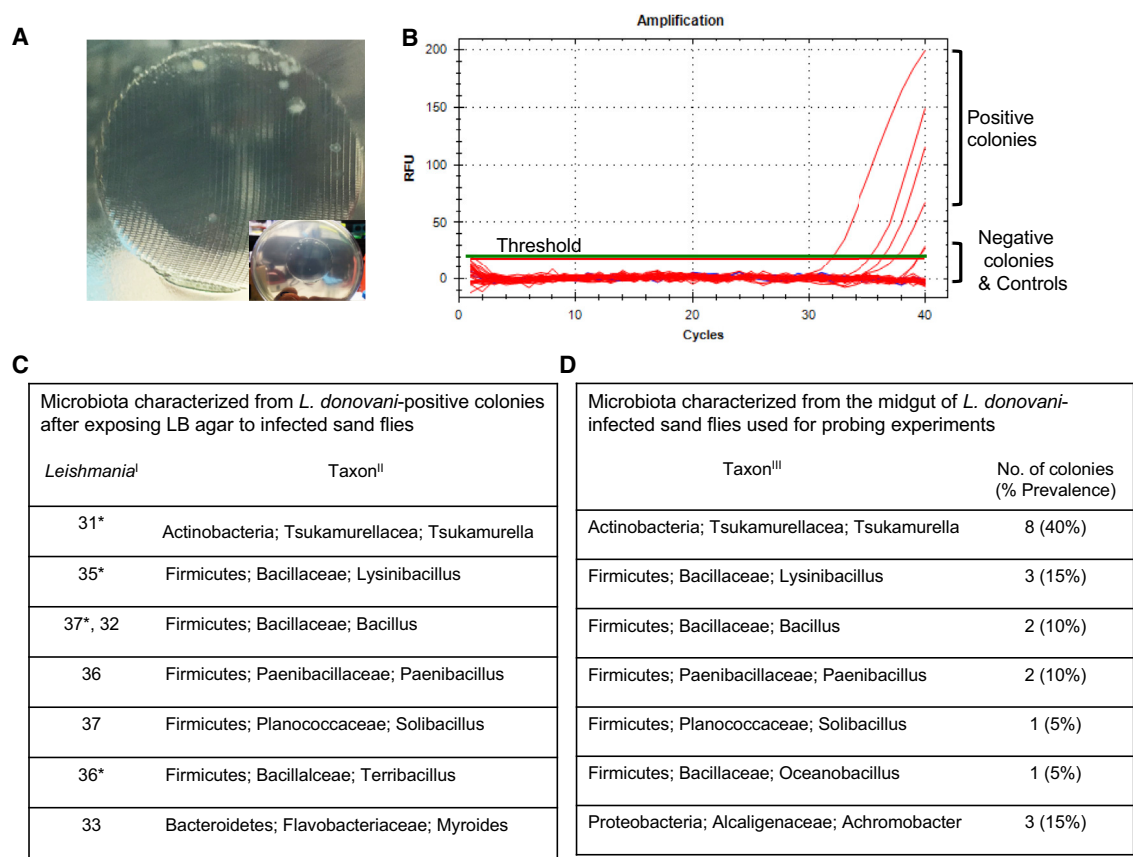
Figure 3. Identification of Gut Microbes Egested during Infected Sand Fly Bites

(A) Bacterial colonies growing on LB/agar after exposure to *L. donovani*-infected sand flies. Inset shows the mesh imprint of the feeder containing the sand flies. Pictures are representative of five independent experiments.

(B) Representative real-time PCR amplification curves (red lines) for *Leishmania* minicircle kDNA using bacterial colonies picked from agar plates as template. Green line, threshold; blue lines, negative controls (water or agar).

(C) Bacteria identified from *Leishmania*-positive colonies. I, real-time PCR C_T values for amplified *Leishmania*; II, taxonomy of bacteria ordered by phylum, family, and genus. Asterisks indicate colonies depicted in (B).

(D) Bacteria identified from the midgut of infected sand fly groups used in (A). III, taxonomy of bacteria ordered by phylum, family, and genus.

See also Movie S1.

colonized sand flies (Kelly et al., 2017; Monteiro et al., 2016; Sant'Anna et al., 2012), may be inoculated into host skin. To demonstrate the egestion of midgut microbes during sand fly bites, we exposed infected flies to warmed sterile Luria broth (LB)/agar plates for 1 hr (Movie S1), and allowed the bacteria to grow overnight (Figure 3A). We amplified *Leishmania* DNA from eight screened colonies, providing us with a definitive guide to bite sites (Figure 3B). We then isolated and sequenced bacteria from the *Leishmania*-positive bite sites and from plated midgut colonies of the sand flies (Figures 3C and 3D). Of the genera identified from bite sites, *Tsukamurella*, *Lysinibacillus*, *Paenibacillus*, *Solibacillus*, and *Bacillus* were present in midgut colonies of sand flies used in probing. Importantly, *Tsukamurella*

is also an indicator species that distinguishes microbiota of infected from uninfected midguts (Kelly et al., 2017).

Gut Microbes of Sand Flies Provide the Initial Signal for NLRP3 Priming

To demonstrate that midgut microbes prime the inflammasome, we provided sand flies harboring mature infections with a sugar meal containing an antibiotic cocktail for 36 hr after confirming that it has no adverse effect on the growth or differentiation of *Leishmania* parasites in culture (Figures S3A and 3B). We then demonstrated the efficacy of antibiotic treatment *in vivo* through its significant reduction of the number of cultivable gut microbiota (Figure 4A). We also demonstrated that sand flies given

Figure 4. Diminishing Sand Fly Gut Microbiota Mitigates Inflammasome Activation, Abrogates Neutrophil Recruitment, and Compromises Dissemination of *L. donovani*

In (A)–(L), sand flies harboring mature infections with *L. donovani* were left untreated (IS) or were provided a cocktail of three antibiotics for 36 hr prior to parasite transmission to mouse ears (IS + ATB).

(A) Bacterial colony growth on LB/agar after plating 10 midguts.

antibiotics were similar to controls in their survival (Figure 4B), their support of *Leishmania* growth and differentiation to infective metacyclics (Figure 4C), the virulence of their midgut-resident metacyclics assessed by their ability to invade and replicate within BMDM (Figures 4D and 4E), their feeding behavior (Figure 4F), and their capacity to transmit parasites to mouse ears (Figure 4G).

Diminishing gut microbiota by antibiotic treatment had a significant effect on decreasing the IL-1β protein level after bites when compared with controls (Figure 4H). Additionally, protein levels of NLRP3, pro-caspase-1, and cleaved caspase-1 as well as IL-1β were reduced in skin exposed to antibiotic-treated sand flies compared with controls (Figure 4I and Table S1). Furthermore, NLRP3 levels after immunoprecipitation with ASC were strongly decreased after antibiotic treatment (Figure 4J and Table S1), indicative of the loss of inflammasome assembly. Noteworthy, a prolonged treatment of uninfected sand flies using a stronger antibiotics cocktail also reduced *Il1b* and *Nlrp3* mRNA expression, and IL-1β protein levels, compared with controls (Figures S3C and S3D) despite unaltered fitness of the flies (Figures S3E and S3F). These results provide strong evidence of the role of gut microbes in initiating a potent inflammatory response by their rapid priming of the NLRP3 inflammasome.

Inflammasome-Derived IL-1β Augments Neutrophil Recruitment and Its Absence Disrupts the Establishment of *Leishmania* Infection

To assess the relevance of gut microbiota or inflammasome-derived IL-1β to *L. donovani* infection, we used antibiotic-treated sand flies to transmit parasites to mice, or treated mice with anakinra, an IL-1R antagonist, prior to parasite transmission with untreated infected sand flies (Figures 4K–4N). Due to the focal nature of sand fly bite sites—distinct focal sites of inflammation are visible along the ear section—we used IHC staining to accurately assess the effect of the two treatments on neutrophil recruitment. Both antibiotic treatment of infected sand flies and anakinra treatment of mice abrogated the intense recruitment of neutrophils observed in control mice 6 hr after infected sand fly bites (Figures 4K and 4M). Although we did not track the fate of the parasites at the bite site, both treatments also resulted in a significant decrease in the splenic parasite burden at 3 weeks after infection, an early time point chosen to assess

parasite dissemination from the skin (Figures 4L and 4N). Interestingly, the intradermal co-injection of parasites with either 10³ live *Solibacillus* bacteria (LI + CFU), recovered from a *Leishmania*-positive bite site (Figure 3C), or 1 μg of LPS (LI + LPS) only partially reproduced the immune response after IS (Figure S4). Six hours after co-injection, both *Nlrp3* and *Il1b* were induced to significantly higher levels in mice co-injected with either LI + CFU or LI + LPS compared with parasites alone (LI) (Figure S4A), leading to enhanced neutrophil recruitment (Figure S4B). However, expression of *Ym1*, used as an indicator for M2 Mo/MΦ and *Mmp9*, uniquely induced by IS (Figures 1H and 1I), remained low (Figure S4A), and parasite visceralization to the spleen 3 weeks later was poor (Figure S4C). These data demonstrate that alone, microbe-triggered inflammasome activation and IL-1β production, though required, are insufficient for parasite dissemination, and emphasize the need for other components in the infectious inoculum to initiate the unique inflammatory response observed after IS.

DISCUSSION

The early events governing pathogen establishment at bite sites of arthropod vectors are poorly investigated despite evidence that disease is often enhanced after vector transmission (Liu and Bonnet, 2014; Peters et al., 2008; Pingen et al., 2016). This has mostly been attributed to immunomodulatory components of saliva co-egested with the pathogen into the host (Abdeladhim et al., 2014; Liu and Bonnet, 2014; Schmid et al., 2016). Recent studies have suggested that elements other than saliva may also participate in disease-enhancing features of pathogen transmission by vector bites (Peters et al., 2008; Pingen et al., 2016). Our findings suggest that microbes residing in the gut of the sand fly are egested into the host alongside *Leishmania* and prime the inflammasome to produce significantly higher levels of IL-1β compared with levels induced by parasites alone. Although *Leishmania* parasites have been reported to activate the inflammasome, this phenomenon has only been demonstrated in the presence of LPS (Charmoy et al., 2016; Lima-Junior et al., 2013). Here, we propose that microbes of the arthropod vector are providing the priming signal needed for optimal inflammasome activation in the natural setting of infected vector bites. We theorize that this early burst of microbe-induced IL-1β

(B) Survival of sand flies without (red) and after antibiotic treatment (green).

(C) Parasite burden and percentage of metacyclics in sand flies prior to transmission. Data in (A) to (C) are representative of four independent experiments (n ≥ 9 sand flies per condition per time point).

(D and E) *In vitro* invasion and multiplication of anterior gut-residing parasites from IS or IS + ATB in bone marrow-derived macrophages (BMDM). Data are representative of two independent experiments. (D) BMDM 48 hr after infection. Arrows indicate intracellular *Leishmania* amastigotes. (E) Percentage of infected BMDM and the number of parasites per cell.

(F) Feeding score after parasite transmission to mouse ears. Data are representative of four independent experiments (n = 16 sand flies per condition).

(G–J) Mouse ear lysates after exposure to 20 IS or IS + ATB. (G) Parasite burden determined by qPCR from individual mouse ears 2 hr after bites. (H) *Ex vivo* IL-1β protein levels measured by ELISA 6 hr after bites. Data in (G) and (H) are pooled from two independent experiments (n ≥ 15 mouse ears per condition). (I) Representative western blot of NLRP3, caspase-1, and pro-IL-1β protein levels (n = 2 mouse ears per condition). (J) Representative western blot of NLRP3 protein levels after immunoprecipitation using anti-ASC antibody (n = 2 mouse ears per condition).

(K–N) Mouse ears were exposed to IS or IS + ATB (K and L). Mice were left untreated or were treated with anakinra 12 hr and immediately before exposure to IS (IS + Ana) (M and N). (K and M) Mouse ear sections were stained with anti-Gr1 antibody 6 hr after exposure to IS. Data are representative of two independent experiments (n = 4–5 mouse ears per condition). Scale bars, 50 μm. (L and N) Parasite burden in spleens of individual mice determined by serial dilution 3 weeks after exposure to IS or IS + ATB. Data are pooled from two independent experiments distinguished by solid and clear symbols (n ≥ 8 mice per condition).

Statistical significance (*p < 0.05, **p < 0.01) was calculated using the unpaired two-tailed t test (H) and the Wilcoxon ranked sum test (L and N). Error bars indicate the geometric mean with 95% confidence interval for parasite burden (C, G, L, and N), the mean ± SEM (B), and percentage of metacyclics (C, E, F, and H). See also Figure S4 and Table S1.

provides an autocrine signal for further recruitment of neutrophils following vector transmission of *Leishmania* amplifying the response. Of note, sand flies harboring mature *Leishmania* infections exhibit altered feeding behavior with prolonged probing and increased feeding persistence (Rogers, 2012). This can potentially lead to more cell damage at the bite site. As such, the higher levels of mature IL-1β observed after infected sand fly bites could partly involve extracellular processing of immature IL-1β by neutrophil and mast cell-derived proteases (Afonina et al., 2015; Opdenakker et al., 2001). Indeed, mast cell degranulation, infiltration of neutrophils, and *Mmp9* induction were all significantly higher after infected compared with uninfected sand fly bites.

The intensified and prolonged recruitment of neutrophils after bites of *L. donovani*-infected sand flies resembles the response described following bites of *L. major*-infected *Phlebotomus duboscqi* (Peters et al., 2008). Since loss of neutrophils also significantly compromises *L. donovani* infection, we theorize that, similar to *L. major* (Peters et al., 2008), neutrophils likely play a part in shielding *L. donovani* parasites and promoting infection of macrophages post transmission.

Increased recruitment of neutrophils was also observed following bites of virus-infected mosquitoes (Pingen et al., 2016). Importantly, this response led to enhanced viral establishment and dissemination caused by the enriched number of virus-susceptible myeloid cells arriving at the bite site. In the present study, a remarkably similar effect was observed for vector-transmitted *L. donovani*. After infected sand fly bites, successful dissemination of parasites to internal organs was associated with an intensified and prolonged recruitment of both neutrophils and inflammatory monocytes to the bite site. This led us to hypothesize that microbe-mediated enhancement of the inflammatory response, through its activation of the inflammasome, facilitate downstream events that govern parasite dissemination to internal organs. A significant reduction in parasite burden following transmission by antibiotic-treated infected sand flies, which was also associated with poor infiltration of neutrophils, supports this hypothesis. It is important to underscore, however, that microbe-mediated neutrophil recruitment, though required, is not directly responsible for parasite dissemination. Whether microbes are involved in governing the early response to infected mosquito bites remains to be proven. However, the documented presence of bacteria in salivary glands of several mosquito species (Sharma et al., 2014; Tchioffo et al., 2015), combined with the fact that multiple pathogens are transmitted in saliva after they colonize the salivary glands, suggests that this may be possible.

Skin represents the first barrier against invading pathogens. Once breached, skin cells of the epidermis and dermis collaborate to release an array of mediators aimed at tissue repair and healing. This universal innate response involves sequential steps that are fine-tuned to produce a self-limiting inflammation involving a transient recruitment of neutrophils and monocytes to the site of injury, aimed at clearing damaged cells and foreign invaders and initiating tissue remodeling and wound repair (de Oliveira et al., 2016; Murray and Wynn, 2011). Considering that most arthropod vectors contain a rich microbial community in several tissues including the gut and salivary glands, and some such as ticks transmit several bacteria of medical importance

(Berggoetz et al., 2014; Monteiro et al., 2016; Qiu et al., 2014; Sant'Anna et al., 2012; Sharma et al., 2014), vector-borne pathogens may have evolved mechanisms to enhance recruitment neutrophils and monocytes, the main cellular arms of this response (Peters et al., 2008; Pingen et al., 2016).

Microbial communities of vectors may vary according to environment and biotope, and the relevance of microbial diversity in induction of the inflammasome needs to be addressed. However, since a wide range of bacterial species efficiently prime the promiscuous NLRP3 inflammasome (Guo et al., 2015), we theorize that variations in microbial communities may have more of a quantitative than a qualitative effect on its activation potentially influencing the severity of disease. We therefore propose that the mechanism put forward here for the sustained recruitment of neutrophils is a central one that occurs in most if not all events that follow *Leishmania*-infected sand fly bites, and potentially bites of other infected vectors.

In sum, our collective data show that vector transmission of *Leishmania* parasites initiates a unique sustained immune response at the bite site. We reveal a mechanism triggered by midgut microbiota that acts during the early hours after infected bites, affecting the course of infection. Our data indicate that midgut microbes are egested during infected sand fly bites and initiate an early pro-inflammatory response via inflammasome activation and IL-1β production that is necessary for intense and sustained recruitment of neutrophils to the bite site. Furthermore, we show that this early inflammatory response facilitates downstream events that govern successful visceralization of *L. donovani* parasites. As such these early responses, occurring only following vector transmission of parasites, promote the establishment of leishmaniasis. This puts a renewed emphasis on the importance of vector sand flies in the pathogenesis of leishmaniasis, and the assessment of the efficacy of vaccine candidates. Importantly, the significance of vector microbiota likely transcends sand flies and leishmaniasis with analogous ramifications for other vector-borne diseases.

STAR★METHODS

Detailed methods are provided in the online version of this paper and include the following:

- KEY RESOURCES TABLE
- CONTACT FOR REAGENT AND RESOURCE SHARING
- EXPERIMENTAL MODEL AND SUBJECT DETAILS
    - Mice
    - Parasites
    - Sand Flies
- METHODS DETAILS
    - Sand Fly Infections
    - Antibiotic Treatment of Sand Flies
    - Pre-transmission Scoring
    - Transmission of *L. donovani* via Sand Fly Bites
    - Scoring of Blood-Fed Sand Flies
    - Preparation of Sand Fly Salivary Gland Homogenate
    - Infection of Mice by Needle Injection
    - ELISA, Western Blot and Co-immunoprecipitation Analyses
    - Flow Cytometry of Ear Tissue Cells

- ○ *In Vivo* Blocking of IL1β
- ○ *In Vitro* Measurement of IL1β and IL-10 in Cultures of Bone-Marrow-Derived Macrophages (BMDM)
- ○ *In Vitro* Invasion of BMDM by Gut-Residing Parasites
- ○ Parasite Load Determination by Quantitative PCR
- ○ Parasite Load Determination by Serial Dilution
- ○ Reverse-transcriptase Quantitative PCR
- ○ Immunohistochemical and TUNEL Staining of Ear Tissue
- ○ Exposure of Infected Flies to LB/Agar
- ○ Plating of Midgut Microbiota
- ○ Amplification, Cloning and Sequence Identification of Bacterial DNA
- ○ Infection of Mice by Co-injection of *Leishmania* and Live Bacteria or LPS
- ● QUANTIFICATION AND STATISTICAL ANALYSIS
  - ○ Sample Sizes
  - ○ Statistical Analysis

SUPPLEMENTAL INFORMATION

Supplemental Information includes four figures, two tables, and one movie and can be found with this article online at https://doi.org/10.1016/j.chom.2017.12.002.

AUTHOR CONTRIBUTIONS

Conceptualization, R. Dey, F.O., J.G.V., and S. Kamhawi; Methodology, R. Dey, F.O., and J.G.V., and S. Kamhawi; Investigation, R. Dey, A.B.J., F.O., L.P., A.B.G.-C., T.D.S., W.d.C., P.B., I.V.C.-A., S.T., H.A., A.P., S. Karmakar, N.I., and M.K.; Resources, C.M. and R. Duncan; Writing, R. Dey, F.O., H.L.N., J.G.V., and S. Kamhawi.

DECLARATION OF INTERESTS

The authors declare no competing interests.

REFERENCES

Abdeladhim, M., Kamhawi, S., and Valenzuela, J.G. (2014). What's behind a sand fly bite? The profound effect of sand fly saliva on host hemostasis, inflammation and immunity. Infect. Genet. Evol. *28*, 691–703.

Afonina, I.S., Muller, C., Martin, S.J., and Beyaert, R. (2015). Proteolytic processing of interleukin-1 family cytokines: variations on a common theme. Immunity *42*, 991–1004.

Atayde, V.D., Aslan, H., Townsend, S., Hassani, K., Kamhawi, S., and Olivier, M. (2015). Exosome secretion by the parasitic protozoan *Leishmania* within the sand fly midgut. Cell Rep. *13*, 957–967.

Berggoetz, M., Schmid, M., Ston, D., Wyss, V., Chevillon, C., Pretorius, A.M., and Gern, L. (2014). Protozoan and bacterial pathogens in tick salivary glands in wild and domestic animal environments in South Africa. Ticks Tick Borne Dis. *5*, 176–185.

Bradley, L.M., Douglass, M.F., Chatterjee, D., Akira, S., and Baaten, B.J. (2012). Matrix metalloprotease 9 mediates neutrophil migration into the airways in response to influenza virus-induced toll-like receptor signaling. PLoS Pathog. *8*, e1002641.

Charmoy, M., Hurrell, B.P., Romano, A., Lee, S.H., Ribeiro-Gomes, F., Riteau, N., Mayer-Barber, K., Tacchini-Cottier, F., and Sacks, D.L. (2016). The Nlrp3 inflammasome, IL-1beta, and neutrophil recruitment are required for susceptibility to a non-healing strain of *Leishmania major* in C57BL/6 mice. Eur. J. Immunol. *46*, 897–911.

Chiba, N., Shimada, K., Chen, S., Jones, H.D., Alsabeh, R., Slepenkin, A.V., Peterson, E., Crother, T.R., and Arditi, M. (2015). Mast cells play an important role in chlamydia pneumoniae lung infection by facilitating immune cell recruitment into the airway. J. Immunol. *194*, 3840–3851.

Cox, J., Mota, J., Sukupolvi-Petty, S., Diamond, M.S., and Rico-Hesse, R. (2012). Mosquito bite delivery of dengue virus enhances immunogenicity and pathogenesis in humanized mice. J. Virol. *86*, 7637–7649.

De Filippo, K., Dudeck, A., Hasenberg, M., Nye, E., van Rooijen, N., Hartmann, K., Gunzer, M., Roers, A., and Hogg, N. (2013). Mast cell and macrophage chemokines CXCL1/CXCL2 control the early stage of neutrophil recruitment during tissue inflammation. Blood *121*, 4930–4937.

de Oliveira, S., Rosowski, E.E., and Huttenlocher, A. (2016). Neutrophil migration in infection and wound repair: going forward in reverse. Nat. Rev. Immunol. *16*, 378–391.

Gomes, R., and Oliveira, F. (2012). The immune response to sand fly salivary proteins and its influence on leishmania immunity. Front. Immunol. *3*, 110.

Guarda, G., Braun, M., Staehli, F., Tardivel, A., Mattmann, C., Forster, I., Farlik, M., Decker, T., Du Pasquier, R.A., Romero, P., and Tschopp, J. (2011). Type I interferon inhibits interleukin-1 production and inflammasome activation. Immunity *34*, 213–223.

Guo, H., Callaway, J.B., and Ting, J.P. (2015). Inflammasomes: mechanism of action, role in disease, and therapeutics. Nat. Med. *21*, 677–687.

Gurung, P., Karki, R., Vogel, P., Watanabe, M., Bix, M., Lamkanfi, M., and Kanneganti, T.D. (2015). An NLRP3 inflammasome-triggered Th2-biased adaptive immune response promotes leishmaniasis. J. Clin. Invest. *125*, 1329–1338.

Kelly, P.H., Bahr, S.M., Serafim, T.D., Ajami, N.J., Petrosino, J.F., Meneses, C., Kirby, J.R., Valenzuela, J.G., Kamhawi, S., and Wilson, M.E. (2017). The gut microbiome of the vector *Lutzomyia longipalpis* is essential for survival of *Leishmania infantum*. MBio *8*, https://doi.org/10.1128/mBio.01121-16.

Lawyer, P.G., Meneses, C., Rowland, T., and Rowton, E.D. (2016). Care and Maintenance of Phlebotomine Sand Flies (Walter Reed Army Institute of Research and BEI Resources), p. 62.

Lima-Junior, D.S., Costa, D.L., Carregaro, V., Cunha, L.D., Silva, A.L., Mineo, T.W., Gutierrez, F.R., Bellio, M., Bortoluci, K.R., Flavell, R.A., et al. (2013). Inflammasome-derived IL-1beta production induces nitric oxide-mediated resistance to *Leishmania*. Nat. Med. *19*, 909–915.

Liu, X.Y., and Bonnet, S.I. (2014). Hard tick factors implicated in pathogen transmission. PLoS Negl. Trop. Dis. *8*, e2566.

Monteiro, C.C., Villegas, L.E., Campolina, T.B., Pires, A.C., Miranda, J.C., Pimenta, P.F., and Secundino, N.F. (2016). Bacterial diversity of the American sand fly *Lutzomyia intermedia* using high-throughput metagenomic sequencing. Parasit. Vectors *9*, 480.

Murray, P.J., and Wynn, T.A. (2011). Protective and pathogenic functions of macrophage subsets. Nat. Rev. Immunol. *11*, 723–737.

Opdenakker, G., Van den Steen, P.E., Dubois, B., Nelissen, I., Van Coillie, E., Masure, S., Proost, P., and Van Damme, J. (2001). Gelatinase B functions as regulator and effector in leukocyte biology. J. Leukoc. Biol. *69*, 851–859.

Peters, N.C., Egen, J.G., Secundino, N., Debrabant, A., Kimblin, N., Kamhawi, S., Lawyer, P., Fay, M.P., Germain, R.N., and Sacks, D. (2008). In vivo imaging reveals an essential role for neutrophils in leishmaniasis transmitted by sand flies. Science *321*, 970–974.

Pingen, M., Bryden, S.R., Pondeville, E., Schnettler, E., Kohl, A., Merits, A., Fazakerley, J.K., Graham, G.J., and McKimmie, C.S. (2016). Host inflammatory response to mosquito bites enhances the severity of arbovirus infection. Immunity *44*, 1455–1469.

Porta, C., Rimoldi, M., Raes, G., Brys, L., Ghezzi, P., Di Liberto, D., Dieli, F., Ghisletti, S., Natoli, G., De Baetselier, P., et al. (2009). Tolerance and M2 (alternative) macrophage polarization are related processes orchestrated by p50 nuclear factor kappaB. Proc. Natl. Acad. Sci. USA *106*, 14978–14983.

Qiu, Y., Nakao, R., Ohnuma, A., Kawamori, F., and Sugimoto, C. (2014). Microbial population analysis of the salivary glands of ticks; a possible strategy for the surveillance of bacterial pathogens. PLoS One *9*, e103961.

Radwan, M., Stiefvater, R., Grunert, T., Sharif, O., Miller, I., Marchetti-Deschmann, M., Allmaier, G., Gemeiner, M., Knapp, S., Kovarik, P., et al. (2010). Tyrosine kinase 2 controls IL-1ss production at the translational level. J. Immunol. *185*, 3544–3553.

Ribeiro-Gomes, F.L., and Sacks, D. (2012). The influence of early neutrophil-*Leishmania* interactions on the host immune response to infection. Front. Cell. Infect. Microbiol. *2*, 59.

Rogers, M.E. (2012). The role of leishmania proteophosphoglycans in sand fly transmission and infection of the mammalian host. Front. Microbiol. *3*, 223.

Sant'Anna, M.R., Darby, A.C., Brazil, R.P., Montoya-Lerma, J., Dillon, V.M., Bates, P.A., and Dillon, R.J. (2012). Investigation of the bacterial communities associated with females of *Lutzomyia* sand fly species from South America. PLoS One *7*, e42531.

Schmid, M.A., Glasner, D.R., Shah, S., Michlmayr, D., Kramer, L.D., and Harris, E. (2016). Mosquito saliva increases endothelial permeability in the skin, immune cell migration, and dengue pathogenesis during antibody-dependent enhancement. PLoS Pathog. *12*, e1005676.

Sharma, P., Sharma, S., Maurya, R.K., Das De, T., Thomas, T., Lata, S., Singh, N., Pandey, K.C., Valecha, N., and Dixit, R. (2014). Salivary glands harbor more diverse microbial communities than gut in *Anopheles culicifacies*. Parasit. Vectors *7*, 235.

Shi, C., and Pamer, E.G. (2011). Monocyte recruitment during infection and inflammation. Nat. Rev. Immunol. *11*, 762–774.

Shimada, K., Crother, T.R., Karlin, J., Dagvadorj, J., Chiba, N., Chen, S., Ramanujan, V.K., Wolf, A.J., Vergnes, L., Ojcius, D.M., et al. (2012). Oxidized mitochondrial DNA activates the NLRP3 inflammasome during apoptosis. Immunity *36*, 401–414.

Sica, A., Invernizzi, P., and Mantovani, A. (2014). Macrophage plasticity and polarization in liver homeostasis and pathology. Hepatology *59*, 2034–2042.

Silverman, J.M., and Reiner, N.E. (2011). *Leishmania* exosomes deliver preemptive strikes to create an environment permissive for early infection. Front. Cell. Infect. Microbiol. *1*, 26.

Späth, G.F., and Beverley, S.M. (2001). A lipophosphoglycan-independent method for isolation of infective *Leishmania* metacyclic promastigotes by density gradient centrifugation. Exp. Parasitol. *99*, 97–103.

Tchioffo, M.T., Boissiere, A., Abate, L., Nsango, S.E., Bayibeki, A.N., Awono-Ambene, P.H., Christen, R., Gimonneau, G., and Morlais, I. (2015). Dynamics of bacterial community composition in the malaria mosquito's epithelia. Front. Microbiol. *6*, 1500.

WHO. (2014). A Global Brief on Vector-Borne Diseases (WHO).

STAR★METHODS

KEY RESOURCES TABLE

REAGENT or RESOURCE	SOURCE	IDENTIFIER
Antibodies		
anti-ASC antibody	Santa Cruz Biotech	Cat# sc-22514-R; RRID:AB_2174874
Anti- IL-1β antibody	R&D Systems	Cat# AF-401-NA; RRID:AB_416684
Anti-caspase-1 p-10 (M-20) antibody	Santa Cruz Biotechnology	Cat# sc-514; RRID:AB_2068895
Anti-NLRP3 mAb antibody	AdipoGen	Cat# AG-20B-0006; RRID:AB_2490186
Anti-β-actin	abcam	Cat# ab20272; RRID:AB_445482
donkey anti-goat IgG-HRP antibody	Santa Cruz Biotech	Cat# sc-2056; RRID:AB_631730
goat anti-rabbit IgG HRP antibody	Jackson ImmunoResearch Laboratories	Cat# 111-035-045; RRID:AB_2337938
goat anti-mouse IgG + IgM HRP antibody	Jackson ImmunoResearch Laboratories	Cat# 115-035-068; RRID:AB_2338505
FITC- Ly6C Monoclonal antibody	BD Biosciences	Cat# 553104 ; RRID:AB_394628
PE-Ly6G Monoclonal antibody (Clone 1A8)	BD Biosciences	Cat# 551461; RRID:AB_394208
PE-Cy7 anti-CD11b Monoclonal antibody	BD Biosciences	Cat# 552850 RRID:AB_394491
APC anti-mouse IL-1β pro form antibody (Clone NJTEN3)	eBioscence	Cat# 17-7114-80 RRID:AB_10670739
anti-Ly6G antibody (Clone RB6-8C5)	Thermo Fisher Scientific	Cat# MA1-82776 ;RRID:AB_2295123
anti-macrophage antibody (clone MAC387)	abcam	cat# ab22506; RRID:AB_447111
anti-IL-1β antibody HRP conjugated (mature form)	abcam	cat# ab106035; RRID:AB_10903323
Bacterial and Virus Strains		
Leishmania donovani	MHOM/SD/62/1S	N/A
Solibacillus	This Study	N/A
Chemicals, Peptides, and Recombinant Proteins		
Liberase TL	Roche	Cat# 05401020001
LB/Agar plates	Sigma-Aldrich	Cat# L5542-10EA
Taq PCR Kit	New England BioLabs	Cat# E500S
PCR4-TOPO Vector	ThermoFisher Scientific	Cat# K457502
Anakinra	Amgen	N/A
Cell Lysis Buffer 1X	eBioscience	EPX-99999-000
SuperSignal West Femto Maximum Sensitivity Substrate	ThermoFisher Scientific	Cat# 34095
Penicillin/Streptomycin (cell culture)	Gibco	Cat# 15140-122
Penicillin (Sand fly treatment)	Sigma-Aldrich	Cat# P3032
Gentamycin	Sigma-Aldrich	Cat# PHR1077
Vancomycin	Sigma-Aldrich	Cat# V1130
Doxycycline	Sigma-Aldrich	Cat# D9891
Clindamycin	Sigma-Aldrich	Cat# C5269
LPS	Sigma-Aldrich	Cat# L2654
Critical Commercial Assays		
RNeasy Plus Mini Kits	QIAGEN	Cat# 74134
PureLink RNA Mini kits	Ambion	Cat# 12183018A
DNeasy Blood & Tissue kits	QIAGEN	Cat# 69504
Taqman High-Capacity cDNA Reverse Transcription kit	Life Technologies	Cat# 4368814
GeneJET Plasmid Miniprep Kit	ThermoFisher Scientific	Cat# K0502
Fixable Yellow Dead Cell Stain kit	Invitrogen	Cat# L34959
Mouse IL-1β ELISA Ready-SET-GO! Kits	eBioscience	Cat # 88-7013

Continued

REAGENT or RESOURCE	SOURCE	IDENTIFIER
Mouse IL-10 ELISA Ready-SET-GO! Kits	eBioscience	Cat # 88-7105
Perm/Wash Buffer	BD Biosciences	Cat#51-2091KZ
Experimental Models: Organisms/Strains		
Mouse: BALB/c	Charles River Laboratories	Strain Code # 555
Sand Fly (*Lutzomya longipalpis*)	LMVR/NIAID/NIH	N/A
Oligonucleotides		
16S_27 forward primer 5'-AGA GTT TGA TCC TGG CTC AG-3'	This Study	N/A
16S_27 reverse primer 5'-GGT TAC CTT GTT ACG ACT T-3'	This Study	N/A
Leishmania forward primer 5'-CCTATTTTACACCAACCCCCAGT-3'	This Study	N/A
Leishmania reverse primer 5'-GGGTAGGGGCGTTCTGCGAAA-3'	This Study	N/A
Leishmania probe 5'-RAAARKKVRTRCAGAAAYCCCGT-3'	This Study	N/A
Software and Algorithms		
FlowJo Software 4.3	FlowJO, LLC	http://docs.flowjo.com/vx/
BZII Viewer Software	Keyence	https://www.bioz.com/result/bz%20ii%20viewer%20software/product/KEYENCE
Olympus CellSens Dimension version 1.9	Olympus	https://www.olympus-lifescience.com/en/software/cellsens/
ImageJ.exe Software	NIH	https://imagej.nih.gov/ij/download.html
Prsim software	graphpad	https://www.graphpad.com/scientific-software/prism/

CONTACT FOR REAGENT AND RESOURCE SHARING

Further information and requests for resources and reagents should be directed to and will be fulfilled by the Lead Contact, Shaden Kamhawi (skamhawi@niaid.nih.gov).

EXPERIMENTAL MODEL AND SUBJECT DETAILS

Mice

Six- to eight-week-old female BALB/c mice from Jackson Laboratories were used in experiments. Animals were housed under pathogen-free conditions at the NIAID Twinbrook animal facility in Rockville, MD. Animal group sizes where based on historical studies suitable for observing the effects of vector-transmitted and needle-initiated *Leishmania* infections. Animals were randomly assigned to groups exposed to *Leishmania*-infected sand flies, uninfected sand flies, or chosen for needle injection of parasites with or without salivary glands. All samples were assayed collectively so that the investigator was blind to the specific outcome of an assay for a particular group. All animal experimental procedures were reviewed and approved by the National Institute of Allergy and Infectious Diseases (NIAID) Animal Care and Use Committee under animal protocol LMVR4E. The NIAID DIR Animal Care and Use Program complies with the Guide for the Care and Use of Laboratory Animals and with the NIH Office of Animal Care and Use and Animal Research Advisory Committee guidelines. Detailed NIH Animal Research Guidelines can be accessed at https://oma1.od.nih.gov/manualchapters/intramural/3040-2/.

Parasites

The parasite strain used in this study, *L. donovani* (MHOM/SD/62/1S), was maintained by serial passages in Golden Syrian hamsters. *L. donovani* promastigotes were cultured in Schneider's medium (Gibco-BRL, NY) supplemented with 20% heat-inactivated fetal bovine serum, 2 mM L-glutamine, 100 U/mL penicillin, and 100 μL/mL streptomycin at 26°C.

Sand Flies

Lutzomyia longipalpis sand flies, Jacobina strain, were reared at the Laboratory of Malaria and Vector Research, NIAID, NIH according to protocols provided in ''Care and Maintenance of Phlebotomine Sand flies'' (Lawyer et al., 2016).

METHODS DETAILS

Sand Fly Infections

Two to four-day-old colony-bred *Lu. longipalpi*s females were infected by artificial feeding through a chick membrane on defibrinated rabbit blood (Spring Valley Laboratories, Sykesville, MD) containing 5×10^6 amastigotes of *L. donovani* and 30μl penicillin/streptomycin (10,000 units penicillin/10mg streptomycin) per mL of blood. It is important to note that *L. donovani* amastigotes were isolated from terminally sick hamsters with advanced visceral leishmaniasis (VL), and amastigotes were freshly prepared on the day of infection. Though not required, using fresh parasites from terminally sick hamsters in a VL model of infection reduces the variability during the development of *Leishmania* in individual sand flies. This produces more homogenous mature infections that are optimal for transmission experiments. Fully blood-fed female sand flies were separated and maintained at 26°C with 75% humidity and were provided 30% sucrose until the flies developed a mature infection for transmission.

Antibiotic Treatment of Sand Flies

For antibiotic treatment of uninfected sand flies, females were fed on defibrinated rabbit blood for 3h in the dark. Fully blood-fed females were separated and maintained at 26°C with 75% humidity for 11 days. After separation, half of the blood-fed sand flies were offered a 30% sucrose solution containing 100U/ml Penicillin, 50μg/ml Gentamicin, 20μg/ml Vancomycin, 16μg/ml Doxycycline and 4μg/ml Clindamycin through soaked cotton balls. The second half was offered 30% sucrose. Dead sand flies were removed and counted every three days. For infected sand flies, females were given a weaker antibiotic cocktail of 100U/ml Penicillin, 50μg/ml Gentamicin and 4μg/ml Clindamycin for 36h after the development of mature transmissible infections (on days nine through 11 post-infection). The total parasite load per midgut and percent metacyclics were determined for antibiotic-treated and control sand flies by hemocytometer counts.

Pre-transmission Scoring

The parasite load and percentage of metacyclics per midgut in *L. donovani*-infected sand flies were scored on the day of transmission. Depending on fly availability, 10-20 flies were anesthetized with CO_2, washed in 5% soap solution and rinsed in 1X PBS prior to dissection. Each midgut was macerated with a pestle (Kimble Chase, Vineland, NJ) in an Eppendorf tube containing 50μl of 1X PBS. Based on morphology and movement, the parasite load and the percent metacyclics per midgut were determined using a hemocytometer.

Transmission of *L. donovani* via Sand Fly Bites

Mice were anesthetized by intra-peritoneal administration of ketamine (100mg/kg) with xylazine (10mg/kg). Upon full sedation, LubriFresh ophthalmic ointment (Major Pharmaceuticals) was topically applied to the eyes to prevent corneal dryness. Twenty flies with mature infections were applied either to the left ear of each mouse in experiments involving follow-up of the infection or to both ears for 3-18h time points, using vials with a meshed surface held in place by custom-made clamps. Sand flies were allowed to feed for 2-3h in the dark. Time to analysis was counted starting at midpoint of the exposure to sand flies. Five of 292 ears subjected to bites throughout the study had no evidence of transmission (no fed flies and no signs of probing on the ear) and were excluded from further analyses. For experiments involving follow-up of the course of infection, mice were monitored daily for appearance, level of activity, swelling, pain, and ulceration during the course of infection.

Scoring of Blood-Fed Sand Flies

The percent of blood-fed flies was established for each mouse. The flies were aspirated from vials, anesthetized with CO_2, washed in 5% soap solution, rinsed, and placed in 1X PBS. The number of blood-fed flies was determined by observing them under a stereomicroscope. In the absence of a visible blood meal in any of the sand flies subjected to a single ear, midguts were dissected and inspected microscopically for traces of blood.

Preparation of Sand Fly Salivary Gland Homogenate

Salivary glands were dissected from five- to seven-day old female *Lu. longipalpis* sand flies, sonicated for 3-4 cycles and with 1 min on ice in between, then centrifuged at $12,000 \times g$ for 5 min. The supernatant was collected and used immediately. One gland equivalent of the homogenate was mixed with the metacyclic parasite inoculum for each injection.

Infection of Mice by Needle Injection

L. donovani amastigotes used in sand fly infections were cultured in Schneider's medium (Sigma) supplemented with 20% of inactivated FBS, 2mM L-glutamine, 100 units/ml penicillin, and 100μl/ml streptomycin. After seven to nine days, metacyclic parasites were purified from culture using a Ficoll (Sigma) gradient procedure as described previously (Späth and Beverley, 2001). The left ear of each mouse was injected intradermally with 10^5 metacyclics of *L. donovani* in a volume of 10μl in the absence or presence of an extract of one freshly prepared salivary gland using a 29-gauge needle.

ELISA, Western Blot and Co-immunoprecipitation Analyses

Six hours after sand fly bites, exposed mice ears were harvested and homogenized in Procarta cell lysis buffer (eBioscience) using MagNA Lyser Green Beads (Roche). Tissue was further cleaned by passing through QIAshredder (Qiagen) and gDNA Eliminator (RNeasy Plus Mini Kits, Qiagen) columns. IL1β levels were measured directly from ear lysates using Mouse IL1β ELISA Ready-SET-GO! kits (eBioscience). For co-immunoprecipitation, equal amounts of protein from each sample (150μg) were incubated over-night at 4°C with 1μg of anti-ASC antibody (N-15-R; Santa Cruz Biotech, cat# sc-22514-R), followed by a 4h incubation period at 4°C with Pierce Protein A/G-agarose beads (Thermo Scientific). Beads were washed three times and heated for 5 min at 95°C with 2x reducing sample buffer (Bio-Rad) and the eluted samples were run in 10% Mini-PROTEAN TGX pre-cast gels (Bio-Rad). For western blot analyses, protein concentrations were measured from homogenized tissue lysates, and 35μg of protein from each sample was run in 10% Mini-PROTEAN TGX pre-cast gels (Bio-Rad). All electrophoresed gels were transferred onto PVDF membranes using Trans-Blot Turbo Transfer System (Bio-Rad), and membranes were blocked with 5% NFD milk in 1x PBS-Tween 20 (0.1%). Immu-noblotting was performed using antibodies specific to IL1β (R&D, cat# AF-401-NA; 1:700), caspase-1 p-10 (M-20; Santa Cruz Biotech, cat# sc-514; 1:200), NLRP3 (Adipogen, cat# AG-20B-0006-C100; 1:1000), ASC (N-15-R; Santa Cruz Biotech, cat# sc-22514-R; 1:200) and β-actin (abcam cat# ab20272; 1:5000) antibodies; further immunolabeling was done using donkey anti-goat (Santa Cruz Biotech, cat# sc-2056; 1:3000), goat anti-rabbit (Jackson ImmunoResearch Laboratories, cat# 111-035-045; 1:3000), and goat anti-mouse (Jackson ImmunoResearch Laboratories, cat# 115-035-068; 1:3000) antibodies. Each blot was developed with SuperSignal West Femto Maximum Sensitivity Substrate (Thermo Scientific), and visualized using FluorChem$^@$ Q (Alpha Inno-tech). Exposure times for each western blot varied between 10 to 30 seconds. Captured images were processed and analyzed using Photoshop CS4 (Adobe, Inc.).

For western blots and co-immunoprecipitation assays, band densities were measured using ImageJ Software (NIH). Thereafter, the NLRP3, pro-IL-1β, pro-Caspase 1 and cleaved Caspase band densities were normalized to either actin or ASC band densities (Table S1).

Flow Cytometry of Ear Tissue Cells

Ear pinna dermal sheets were harvested, treated with ethanol, separated using forceps and digested in PBS containing Liberase TL (Roche) at 37°C for 1 h. Digested tissues were homogenized in a tissue homogenizer (Medimachine; BD biosciences) and filtered in a 50 μm strainer. The resulting single cell suspensions were stained for Ly6C (clone AL-21; FITC; BD), Ly6G (clone 1A8; PE; BD), CD11b (clone M1/70; PE-Cy7; BD), and with the Fixable Yellow Dead Cell Stain Kit (Invitrogen), after being incubated with anti-Fc (CD16/32) antibodies to block unspecific binding for 30 min. For intracellular detection of IL-1β, ear cells were blocked and stained with surface markers as mentioned above. Thereafter, cells were fixed and permeabilized with Cytofix/Cytoperm (BD), followed by incubation with anti-mouse IL-1β pro-form antibody (clone NJTEN3, APC; eBioscience). Data were analyzed on a MACSQuant flow cytometer (Mil-tenyi Biotec). Cells were acquired based on forward and side scatter and data analyzed with FlowJo Software 4.3.

In Vivo Blocking of IL1β

Twenty milligrams of Anakinra (Kineret; Amgen) or PBS was administered to mice by intra-peritoneal injection 12h and immediately before transmission by infected sand flies. Mice were euthanized at 6h post-transmission to assess infiltration of neutrophils into the ears, and at three weeks post-transmission to determine the parasite burden in draining lymph nodes and spleens. Anakinra was kindly provided by Dr. Raphaela Goldbach-Mansky (National Institute of Arthritis and Musculoskeletal and Skin Diseases, National Institute of Health).

In Vitro Measurement of IL1β and IL-10 in Cultures of Bone-Marrow-Derived Macrophages (BMDM)

Bone marrow cells were isolated from the femurs and tibias of BALB/c mice. Cells were cultured with RPMI medium containing 10% of fetal bovine serum (FBS) along with 20 ng/ml of M-CSF for 7days. Some wells containing BMDMs were treated with 500ng/ml of LPS (Sigma). After 4h of stimulation cells were washed with RPMI, and infected with stationary-phase *L. donovani* promastigotes in two different ratios 1:5 and 1:10 (BMDM: Parasites). After 6h of incubation cell supernatants were collected and centrifuged to re-move parasites. IL1β (Mouse IL-1 beta ELISA Ready-SET-GO!, Cat No 88-7013, eBiosceince) and IL-10 (Mouse IL-10 ELISA Ready-SET-GO!, Cat No 88-7105, eBioscience) cytokine levels were measured according to manufacturer's instructions.

In Vitro Invasion of BMDM by Gut-Residing Parasites

BMDMs were prepared as described above. After 7 days, cells were infected with *L. donovani* metacyclic parasites isolated from different groups of infected sand flies at a ratio of 1:10 (BMDM: Parasites). After 48h of infection cells were washed, fixed with alcohol, and stained with Giemsa. Intracellular parasite numbers were counted in 300-400 macrophages to calculate the percentage of mac-rophages that were infected by parasites and the mean number of parasites/infected macrophage.

Parasite Load Determination by Quantitative PCR

Immediately after transmission by infected sand flies, mice ears were cut and lysed for DNA purification using DNeasy Blood & Tissue kits (Qiagen). Seventy-five nanograms of sample DNA was used as a template in a Taqman-based quantitative PCR. The target DNA was amplified from a kinetoplast minicircle DNA of the parasite. The sequence of primers is given in the Key Resources Table, with the addition of a fluorescent probe 5′-RAAARKKVRTRCA GAAAYCCCGT-3′ for detection. A Black Hole Quencher moiety is coupled to

the 3′ end and Calfluor Red is coupled to a C6 linker at the 5′ end. The degenerate letter code is according to the Nomenclature Committee of the International Union of Biochemistry (http://www.chem.qmul.ac.uk/iubmb/misc/naseq.html). The fluorescent probe is added to the reaction mixture at a final concentration of 1.5 pmols/μl. Cycling parameters: preheat at 95°C for 180 seconds and then 40 two-step cycles of 95°C for 10 seconds and 55°C for 30 seconds. To evaluate the number of *Leishmania* cells that were represented by a given cycle threshold (Ct) value, a standard curve was constructed by purification of DNA from naïve mice ears spiked with a known number of parasites (Figure S1B).

Parasite Load Determination by Serial Dilution

Mice were euthanized by CO_2 inhalation. The spleen and the lymph node draining the bite sites were removed from each mouse under aseptic conditions. The lymph node was macerated in an Eppendorf tube containing 200μL of complete Schneider's medium. The spleen was cut into small pieces, transferred to a 70μm cell strainer and macerated in 1mL of complete Schneider's medium using the back of a syringe plunger. The parasite burden was quantified from the macerate by limiting dilution assays where the number of viable *Leishmania* parasites in each lymph node or spleen was determined from the highest dilution at which *Leishmania* promastigotes could be grown after 15 days of incubation at 26°C.

Reverse-transcriptase Quantitative PCR

Mice were euthanized at indicated time points after exposure to infected sand flies, non-infected sand flies, or after needle injection. The whole ear was homogenized using MagNA Lyser Green Beads (Roche) and total RNA was extracted using PureLink RNA Mini kits (Ambion). Five hundred nanograms of total RNA was reverse-transcribed into cDNA using random hexamers with the Taqman High-Capacity cDNA Reverse Transcription kit (Life Technologies). Expression of the genes listed in Table S2 was determined using Taqman Gene Expression assays (Applied Biosystems) in the CFX96 Touch Real-Time System (BioRad, Hercules, CA). Expression values were determined by the $2^{-\Delta\Delta Ct}$ method; samples were normalized to GAPDH expression and determined relative to expression values from naïve mice.

Immunohistochemical and TUNEL Staining of Ear Tissue

Mouse ears were fixed in 10% buffered formalin phosphate solution and paraffin embedded according to standard procedures. Slides of consecutive serial sections of bites sites were prepared for immune staining. Paraffin sections were dewaxed and rehydrated prior to staining. Dewaxed sections were incubated with anti-Ly6G antibody, clone RB6-8C5 (Thermo Fisher Scientific, 1:100) for neutrophil staining; anti-macrophage antibody, clone MAC387 (abcam, 1:100); anti-IL1β antibody conjugated with HRP (abcam, cat# ab106035; 1:100) for mature IL1β staining; and the corresponding isotype control antibody for each analyte. All stained sections were counterstained with Hematoxylin. For mast cell staining, dewaxed slides were stained with alcian blue counterstained with safranin. TUNEL reactions were performed on paraffin sections that were dewaxed and rehydrated. Slides were incubated with Tdt, UTP and terminal transferase buffer, washed, and incubated with anti-Dig. Color was developed with Fuchsin and slides were counterstained with Hematoxylin. All of the histochemical and immunohistochemical staining was done by Histoserv Inc, Gaithersburg, MD, USA. Stained sections were analyzed at the Infectious Disease Pathogenesis Section (IDPS), Comparative Medicine Branch (CMB), Division of Intramural Research (DIR), NIAID/ NIH, using an Olympus BX51 microscope. Images were taken with an Olympus DP73 Camera using Olympus cellSens Dimension ver.1.9 software. Mast cell counts were performed using the Keyence BZ-9000 microscope and analyzed with BZ-II Viewer software.

Exposure of Infected Flies to LB/Agar

Twenty *Lu. longipalpis* sand flies with mature transmissible infections were placed in a custom-made feeder with a meshed surface to provide access to sterile LB/Agar plates (Sigma-Aldridge). The meshes were autoclaved whereas the feeders were sterilized overnight in 70% ethanol and left to dry for at least 30 min inside a laminar flow hood where the probing experiments were carried out. The LB/Agar plates were placed on top of each feeder for 2h and were kept warm throughout the experiment by a heating device (SunBeam, Model 828B). The plates were then incubated at 30°C and 5% CO_2 for 24-48h.

Plating of Midgut Microbiota

Depending on the experiment, up to 30 sand fly guts were dissected, washed three times in sterile PBS and macerated with a plastic pestle in 450μl of PBS. The equivalent of 10 guts in 150μl were plated on LB agar plates (KD Medical). The plates were incubated at 28°C for 24-48h.

Amplification, Cloning and Sequence Identification of Bacterial DNA

Colonies growing in LB/agar plates after exposure to infected sand flies were picked with a sterile pipet tip and transferred to 30uL of sterile molecular biology grade water. An aliquot was transferred to Luria broth (LB) and bacteria was incubated at 28°C overnight and a glycerol stock was prepared from the culture and stored at -70°C. Water containing the bacteria (5 μl) was used as a DNA template for a PCR reaction using 16S PCR primers (16S_27 forward primer: 5′-AGA GTT TGA TCC TGG CTC AG-3′) and 16S_27 reverse primer: 5′-GGT TAC CTT GTT ACG ACT T-3′), Taq DNA Polymerase (New England BioLabs), 10mM dNTP Mix (Promega) and Molecular Biology Grade Water (Corning). PCR conditions started with denaturation at 95°C for 5 min followed by 35 cycles of denaturation at 95°C for 1 min, annealing at 55°C for 1 min, and extension at 72°C for 1min. Final extension at 72°C was allowed to run for

10 min. Amplicons were visualized by gel electrophoresis with a 1.5% agarose gel (UltraPure Agarose - invitrogen) in 1X TAE buffer (Quality Biological). The PCR product was cloned directly into the PCR4-TOPO Vector (ThermoFisher Scientific) following manufacturing specifications. Plasmids of positive clones were isolated using the GeneJet Plasmid Miniprep Kit (Thermo Scientific) and sequenced at Eurofins MWG Operon using M13 Forward and M13 Reverse primers. Sequences were analyzed using the DNASTAR package (Lasergene) and identified using the NCBI blastn.

Infection of Mice by Co-injection of *Leishmania* and Live Bacteria or LPS

Mice ears were co-injected intradermally with 10^5 metacyclics of *L. donovani* and 10^3 live *Solibacillus* bacteria or $1\mu g$ of LPS in a total volume of $10\mu l$. After identification of *Solibacillus* from a *Leishmania*-positive egestion bite site, the agar bacterial colony was transferred to 30uL of sterile molecular biology grade water. An aliquot was transferred to LB and grown overnight at 28°C and an aliquot was stored as a glycerol stock. A sample of the bacteria was sequenced to confirm the identity of *Solibacillus* and to ensure that it was the only species present in the preparation. Further, a standard curve was established for the number of bacteria by counting colonies plated at various dilutions and optical densities (ODs). For co-injection, *Solibacillus* was grown in Luria broth overnight at 28°C. On the day of injection, $100\mu l$ of bacteria was inoculated into 5ml of fresh Luria broth and growth was monitored hourly until it reached an OD_{600nm} of 0.15. The culture was then diluted with LB medium according to the predetermined standard curve to give 10^3 cfu per $5\mu l$. As for LPS (Lipopolysaccharides from *Escherichia coli* O26:B6, Sigma), the stock solution (2mg/ml) was diluted to $200\mu g/ml$ immediately before use. For co-injection, $5\mu l$ containing 10^5 *L. donovani* metacyclics was mixed with $5\mu l$ of either 10^3 live *Solibacillus* bacteria or $1\mu g$ of LPS.

QUANTIFICATION AND STATISTICAL ANALYSIS

Sample Sizes

n represents the number of mice, mice ears or sand flies as described in legends of each figure.

Statistical Analysis

Data of parasite numbers are portrayed as geometric means with 95% CI; all other data are portrayed as means with SEM or SD. As parasite numbers in the ear of mice transmitted by infected sand flies bites do not follow a Gaussian distribution, we used the stratified Wilcoxon rank sum test to measure significance values from any data related to splenic parasite burden. To compare multiple groups, one-way ANOVA followed by a Holm-Sidak multiple comparisons test was performed. To compare the number of neutrophils in the ear after IS compared to resting skin, we used the Mann-Whitney test. All other significance values were determined using the two-tailed Student's t test. Statistical tests were performed using GraphPad Prism 5.0 software.